Current filaments in turbulent magnetized plasmas

2009 Plasma Phys. Control. Fusion 51 124053

(http://iopscience.iop.org/0741-3335/51/12/124053)

Plasma Phys. Control. Fusion **51** (2009) 124053 (11pp) doi:10.1088/0741-3335/51/12/124053

Current filaments in turbulent magnetized plasmas

E Martines[1], N Vianello[1], D Sundkvist[2], M Spolaore[1], M Zuin[1], M Agostini[1], V Antoni[1], R Cavazzana[1], C Ionita[3], M Maraschek[4], F Mehlmann[3], H W Müller[4], V Naulin[5], J J Rasmussen[5], V Rohde[4], P Scarin[1], R Schrittwieser[3], G Serianni[1], E Spada[1], the RFX-mod team and the ASDEX Upgrade team

[1] Consorzio RFX, Associazione Euratom-ENEA sulla Fusione, Padova, Italy
[2] Space Sciences Laboratory, University of California at Berkeley, Berkeley, CA, USA
[3] Association EURATOM/ÖAW, Institute for Ion Physics and Applied Physics, University of Innsbruck, Innsbruck, Austria
[4] Max-Planck-Institut für Plasmaphysik, EURATOM Association, Garching, Germany
[5] Association EURATOM/RISØ-Technical University of Denmark, Roskilde, Denmark

E-mail: emilio.martines@igi.cnr.it

Received 19 June 2009, in final form 20 July 2009
Published 12 November 2009
Online at stacks.iop.org/PPCF/51/124053

Abstract
Direct measurements of current density perturbations associated with non-linear phenomena in magnetized plasmas can be carried out using *in situ* magnetic measurements. In this paper we report such measurements for three different kinds of phenomena. Current density fluctuations in the edge density gradient region of a fusion plasma confined in reversed field pinch configuration and in a density gradient region in the Earth magnetosphere are measured and compared, showing that in both environments they can be attributed to drift-Alfvén vortices. Current structures associated with reconnection events measured in a reversed field pinch plasma and in the magnetosheath are detected and compared. Evidence of current filaments occurring during ELMs in an H-mode tokamak plasma is displayed.

(Some figures in this article are in colour only in the electronic version)

1. Introduction

Turbulence is ubiquitous in magnetized plasmas, both in nature and in the laboratory. A well-known feature of neutral fluid turbulence is the absence of self-similarity across scales, which takes the name of intermittency [1]. Intermittency manifests itself as a tendency to develop strong tails in the fluctuation probability distribution function (PDF) when going towards small time/spatial scales. The strong events in the PDF tails are due to the formation of localized coherent structures (eddies). Intermittency can also be found in magnetized plasma turbulence, for example in solar wind MHD turbulence [2] and in both electrostatic [3] and

magnetic fluctuations [4] measured in the edge region of fusion devices. Indeed, it is now widely accepted that anomalous transport in the edge of toroidal and linear plasma devices can be caused by the effect of coherent structures, generally labelled as 'blobs', which can undergo a radial motion, convectively carrying energy to the wall. It has been shown that such structures are responsible for the presence of strong tails in the fluctuation PDFs at small scales.

In this paper we present some examples of *in situ* direct measurements of electromagnetic coherent structures. In particular, emphasis is placed on the measurement of field-aligned current density perturbations, obtained from magnetic field measurements. It is shown that this technique, when applicable, allows a great deal of insight into the physical nature of the observed phenomena. The examples shown refer to data already published elsewhere, with emphasis laid on the comparison of similar phenomena observed in different environments.

2. Measurement techniques

This paper deals with current structures measured in magnetized plasmas pertaining to different environments. The systems object of our analysis are the following:

- The edge region of the RFX-mod toroidal device for the confinement of fusion-relevant plasmas in reversed field pinch (RFP) configuration.
- The Earth magnetosphere and the associated magnetosheath created by its interaction with the solar wind.
- The scrape-off layer (SOL) region of the ASDEX Upgrade toroidal device which confines fusion-relevant plasmas in tokamak configuration.

RFX-mod is the largest device in the world operating in RFP configuration [5]. It is designed to explore the scaling of the RFP confinement properties at plasma currents up to 2 MA. It has a major radius $R = 2$ m and a minor radius $a = 0.459$ m, with a circular cross-section, and operates in hydrogen. No limiters or divertors are present, and the last closed flux surface (LCFS) is usually defined by the plasma touching the first wall, which is fully covered by graphite tiles.

ASDEX Upgrade is a mid-size tokamak [6]. It reaches a maximum plasma current of 1.6 MA with a maximum toroidal field of 3.1 T. Its major radius is $R = 1.65$ m and the minor radius is $a = 0.5$ m. The plasma is D-shaped, with a typical elongation of 1.8 and with a single null divertor handling the particle and power exhaust.

The magnetosphere is a region of naturally occurring plasma in the near Earth space environment, dominated by the planetary magnetic field of the Earth. It is a low density collisionless plasma comprising mostly hydrogen, but also minor components of heavier ions originating in the ionosphere as well as the solar wind. The low density and relatively strong magnetization result in an intermediate ratio of kinetic to magnetic pressure, $m_e/m_i < \beta < 1$, in the outer magnetosphere. The magnetospheric plasma often locally exhibits turbulence. The magnetosheath is the shocked solar wind just upstream of the magnetospheric boundary layer. The magnetosheath plasma is of slightly higher density but with lower ambient magnetic field convected from the sun, resulting in a high $\beta > 1$. The magnetosheath is in a highly turbulent state, with naturally occurring current sheets [7, 8].

In all these systems the measurements described have been obtained by means of *in situ* detectors. This kind of measurement, while being perturbative to some extent, allows one to capture the desired quantity at a single point, as an average over a volume much smaller than the typical length scales of the phenomena under consideration. This fact allows one to obtain measurements with an adequate spatial and time resolution.

In RFX-mod a complex probe, dubbed 'U-probe', is used to characterize the electromagnetic features of the edge turbulence [9]. It consists of two boron nitride cases, each of them housing 5×8 electrostatic pins radially spaced by 6 mm. The pins are used as five-pin balanced triple probes [10], allowing the simultaneous measurement of plasma density, electron temperature, electron pressure, plasma potential and their radial profiles at the same toroidal location, as well as the radial and toroidal components of the $\boldsymbol{E} \times \boldsymbol{B}$ plasma velocity. The particular arrangement of electrostatic measurements allows a direct estimate of the local fluctuation of vorticity $\omega = \nabla \times \boldsymbol{v}$, where $\boldsymbol{v}$ is the electric drift velocity, from the floating potential ones V_f, used as a proxy for the plasma potential [11], as $\omega_\parallel = (1/B)\nabla_\perp^2 V_\mathrm{f}$. A radial array of seven tri-axial magnetic coils is located in each case, in order to measure the fluctuations of the three magnetic-field components. Thus a direct estimate of the parallel current density can be made from Ampere's law $j_\parallel \simeq j_\theta = (1/\mu_0)(\partial_\phi b_r - \partial_r b_\phi)$, virtually in the same toroidal position of the vorticity measurements. The data are sampled at a frequency of 5 MHz, while the measurement bandwidth is around 700 kHz. The presented data have been obtained in discharges with a plasma current of 350–400 kA.

The magnetospheric and magnetosheath plasma data have been obtained by the Cluster multi-spacecraft mission [12]. The Cluster flotilla consists of four identical spinning spacecraft flying in a roughly tetrahedron constellation. Each spacecraft is equipped with instruments for sampling of electric and magnetic fields as well as *in situ* particle distribution functions. The electric field experiment consists of spherical Langmuir probes mounted on wire booms with a tip-to-tip length of 88 m. Two such antennas in the spin-plane, with a total of four Langmuir probes, make it possible to measure two components of the three-dimensional electric field from dc (quasi-static) up to a sampling frequency limited in practice only by telemetry rates. The third component is most often unknown. As a by-product the plasma density can be estimated from the spacecraft potential and sampled at 5 Hz. The three components of the magnetic field from dc to 5 Hz are measured by a flux gate magnetometer. The electron and proton temperatures are calculated as moments of the distribution functions, which are sampled every 4 s (the spin-period of the spacecraft). Currents with sampling rates higher than the spin-period and spatial resolution better than the inter-spacecraft distance can be derived implicitly from the low frequency Ampere's law $\boldsymbol{j} = 1/\mu_0 \nabla \times \boldsymbol{B}$, and converting the spatial derivatives to time derivatives by assuming that plasma structures are time-stationary while crossing the spacecraft, possible due to fast convection speeds.

Finally, the data from the ASDEX Upgrade tokamak have been obtained using a reciprocating probe inserted horizontally in the outer mid-plane. The probe head, a cylindrical graphite case of about 60 mm diameter and 115 mm length, is equipped with six electrostatic pins made of graphite (1 mm diameter, 2 mm length) on the front side and a triaxial magnetic probe located 20 mm behind. The probes are arranged to measure the radial and poloidal electric field components from floating potential gradients and the ion saturation current from a single negatively biased pin, while the last pin was used as a sweeping single probe. The magnetic sensors are the same as used in the RFX-mod U-probe, with a measured bandwidth of 1 MHz with -3 dB cutoff at 1.1 MHz. The frequency response of the probe is limited by the graphite shielding to a few tens of kilohertz. The probe was inserted 12 mm in front of the limiter position for 100 ms. The presented data have been obtained with a toroidal magnetic field of 2.5 T, 0.8 MA of plasma current, an on-axis density of $6.5 \times 10^{19}\ \mathrm{m}^{-3}$ and $q_{95} = 5.2$.

3. Drift-Alfvén vortices in magnetized plasmas

Drift waves, in their simplest form, are low frequency waves ($\omega \ll \omega_\mathrm{ci}$, where $\omega_\mathrm{ci} = eB/m_\mathrm{i}$ is the ion cyclotron frequency) which take place in a strongly magnetized plasma with a

cross-field density gradient. They are due to the fact that the plasma responds to a local density perturbation and to the associated potential perturbation due to the electron force balance (Boltzmann's relation) along the magnetic field direction z with an $\boldsymbol{E} \times \boldsymbol{B}$ drift, in quadrature with the perturbation itself. The component of this drift in the direction x of the background density gradient would give rise to a finite divergence of the perturbed particle flux, which is balanced by a propagation of the density perturbation in the third direction (y). The propagation occurs at the electron diamagnetic drift speed $v_{\mathrm{de}} = T_{\mathrm{e}}/(eBL_n)$, L_n being the density gradient scale length $1/L_n = (\mathrm{d}n/\mathrm{d}x)/n$, so that the basic dispersion relation for this kind of waves is $\omega = k_y v_{\mathrm{de}}$.

The electron dynamics parallel to the magnetic field in drift waves is actually modified with respect to Boltzmann's relation by the other terms in the equation of motion. In low β plasmas ($\beta \ll m_{\mathrm{e}}/m_{\mathrm{i}}$, i.e. $\beta \ll 5 \times 10^{-4}$ for a hydrogen plasma) the main modification comes either from collisions with ions or neutrals or from inertia in low-collisionality plasmas. At intermediate β ($m_{\mathrm{e}}/m_{\mathrm{i}} \ll \beta \ll 1$) induction effects are expected to play a dominant role. The parallel drift wave electron currents couple to kinetic Alfvén waves (KAWs), which are an extension of the classic shear Alfvén waves to the domain in which the perpendicular wavelength becomes comparable to the ion gyroradius at electron temperature $\rho_{\mathrm{s}} = c_{\mathrm{s}}/\omega_{\mathrm{ci}}$ [13, 14], where $c_{\mathrm{s}} = \sqrt{T_{\mathrm{e}}/m_{\mathrm{i}}}$ is the ion sound speed. Thus, increasing β a transition occurs from collisional drift waves to drift-Alfvén waves [15]. It is worth mentioning that the condition $\beta \gg m_{\mathrm{e}}/m_{\mathrm{i}}$ is equivalent to $v_{\mathrm{A}} \ll v_{\mathrm{th,e}}$, where $v_{\mathrm{A}} = B/\sqrt{\mu_0 \rho}$ is the Alfvén speed and $v_{\mathrm{th,e}}$ is the electron thermal speed. In both regimes, the non-adiabaticity of electrons gives rise to an instability and causes mass transport down the density gradient due to the associated phase difference between density and potential perturbations. However, in the first case the dynamics is purely electrostatic, whereas at intermediate β values it acquires an electromagnetic character. The corresponding magnetic fluctuations cannot directly contribute to a direct enhancing of cross-field transport through the so-called magnetic flutter transport [16], but are essential for a correct description of the phenomenon.

Drift-Alfvén waves have been shown to be also able to generate in the non-linear phase vortex-like electromagnetic structures, which are named drift kinetic Alfvén (DKA) vortices [17]. DKA vortices, which develop in regions where an average density gradient is present, are a special type of electromagnetic coherent structures [18] displaying the following features: (1) a plasma potential perturbation; (2) a density perturbation almost in phase with the potential one; (3) a field-aligned current density structure; and (4) a vortex-like $\boldsymbol{E} \times \boldsymbol{B}$ plasma motion in the perpendicular plane, occurring at the Alfvén speed, and giving rise to a field-aligned vorticity perturbation.

DKA vortices have been clearly detected in three different kinds of magnetized plasmas, namely in the edge region of the RFX-mod fusion device [19, 20], in the cusp region of the terrestrial magnetosphere [21, 22] and in the VINETA linear plasma device [23]. In the following the results of the first two systems are described and compared. The basic plasma parameters of these two environments are listed in table 1. It can be seen that, despite the differences of many orders of magnitude, the two plasmas are very similar in terms of some non-dimensional parameters. In particular, a β value between 1% and 2% and a ratio ρ_{s}/L_n between 0.1 and 0.2 are found in both systems. On the other hand, the collisionality is very different in the two cases, but this is immaterial for the described phenomenon, as expected in this β range.

The technique used to detect the vortices is different for the two systems. While in RFX-mod the U-probe is stationary with respect to the density gradient region, so that it is immersed in a turbulent layer flowing toroidally, the Cluster spacecrafts fly through the density gradient. So, in the RFX-mod case it is convenient to use a conditional averaging of

Table 1. Plasma parameters for the RFX-mod edge region and for the magnetosphere region where drift-Alfvén vortices have been detected.

Quantity	RFX-mod edge	Magnetosphere
B (T)	0.15	1.7×10^{-7}
n (m^{-3})	1.5×10^{19}	2×10^{6}
T_e (eV)	30	100
T_i (eV)	30 (estim.)	300
$\omega_{ci}/2\pi$ (Hz)	2.3×10^{6}	2.6
ν_{ei} (Hz)	3.3×10^{6}	1.6×10^{-7}
ρ_s (m)	3.7×10^{-3}	6×10^{3}
L_n (m)	0.05	5×10^{4}
v_A ($m\,s^{-1}$)	8.4×10^{5}	2.6×10^{6}
$v_{th,e}$ ($m\,s^{-1}$)	2.3×10^{6}	4.2×10^{6}
v_{de} ($m\,s^{-1}$)	4×10^{3}	1.2×10^{4}
β	0.016	0.012
ρ_s/L_n	0.08	0.21

individual events, in order to extract their basic features from the turbulent background. This is achieved by first performing a wavelet transform of the pressure signal: the wavelet transform amplitude at a given time scale, assumed to correspond to a given spatial scale through the frozen turbulence hypothesis, is used as a trigger for event detection, whenever it exceeds a certain threshold. The averaging of appropriate time windows centered on the trigger time instants for each of the measured quantities yields the typical shape of the structure at the selected scale. In contrast, in the case of the Cluster data, individual events are selected by hand on the time traces, and one of them is shown as a typical example.

The left part of figure 1 shows the average structure detected in the RFX-mod edge region at the radial position $r/a = 0.92$ and at timescale $\tau = 4\,\mu$s. Since the average toroidal flow velocity at this position is $v_\phi = 20\,km\,s^{-1}$, this is equivalent to a spatial scale of 8 cm. The first frame displays the electron pressure perturbation, which is mainly due to a density perturbation [20]. The second frame shows the associated electrostatic potential perturbation, which displays a minimum almost in phase with the pressure peak. This gives rise to an electric field in the perpendicular plane, which is responsible for the vortex-like fluid motion. The structure is actually more complex, because two maxima appear on the two sides of the potential minimum, associated with the local pressure minima. The third frame shows the parallel current density and the parallel vorticity, which both display a peak associated with the pressure peak. Finally, the last two frames display the two components of the $\boldsymbol{E}\times\boldsymbol{B}$ fluid flow in the perpendicular plane. Since the magnetic field at the RFP edge is almost poloidal, these two components are in the toroidal and radial directions, respectively. In the same frames are also shown the corresponding components of the Alfvén velocity, confirming the Alfvénic character of the observed structure. All these observations taken together allow the identification of the structures as DKA vortices. Using the radial array of available measurements, the average structure is found to have a radial size of (2–3)ρ_s. A toroidal size of the magnetic footprint of the order of $100\rho_s$ has been deduced from a toroidal array of in-vessel pick-up coils [19].

The right part of figure 1 depicts a DKA structure observed in the magnetosphere by the Cluster spacecraft, corresponding to the plasma parameters given in table 1. The spacecraft encountered a density gradient around 01:59:10 universal time, shown in panel (a). By using data from all four spacecrafts, information on the density gradient and spatial extension of the vortex can be deduced. However, the sampling rate and sensitivity are not high enough to resolve a density perturbation in the vortex. Only the data obtained by the second

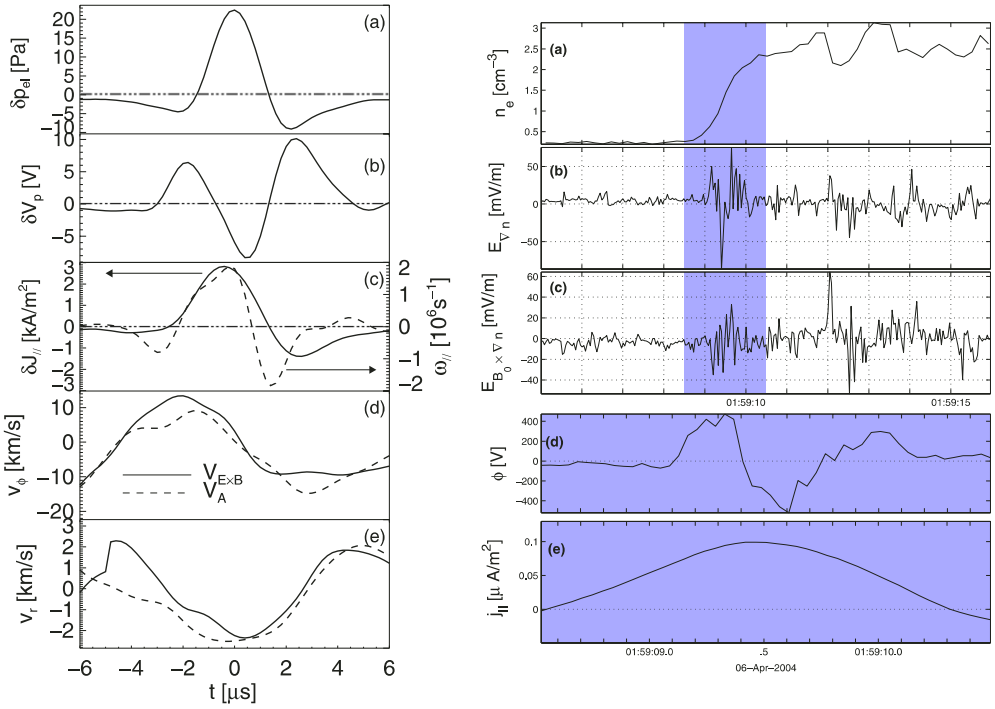

Figure 1. (Left) Average structure detected at timescale $\tau = 4\,\mu$s in the edge region of RFX-mod. From top to bottom are shown the perturbations on (*a*) electron pressure, (*b*) electrostatic plasma potential, (*c*) parallel current density and parallel vorticity (solid and dashed lines, respectively), (*d*) $\boldsymbol{E} \times \boldsymbol{B}$ toroidal velocity and Alfvén velocity (solid and dashed lines, respectively), (*e*) $\boldsymbol{E} \times \boldsymbol{B}$ radial velocity and Alfvén velocity (solid and dashed lines, respectively). (Right) DKA event detected in the magnetosphere. Marked area shows a time period corresponding to a spatial size of $\sim 7\rho_s$. From top to bottom are shown (*a*) density, (*b*) electric field perpendicular to $\boldsymbol{B}_0$ and along density gradient, (*c*) electric field perpendicular to both $\boldsymbol{B}_0$ and density gradient, (*d*) electrostatic plasma potential, (*e*) parallel current density.

spacecraft (C2) are shown. This spacecraft was flying through what is believed to be the center of the vortex. The two perpendicular components of the electric field, along the density gradient $\boldsymbol{E}_{\nabla n}$, and across $\boldsymbol{E}_{\boldsymbol{B}_0 \times \nabla n}$, are shown in panels (*b*) and (*c*), respectively. Since the electric field $\boldsymbol{E}_\perp = -\nabla_\perp \phi$ in the plane perpendicular to the ambient magnetic field is purely electrostatic, it can be integrated to find the electrostatic potential, shown in panel (*d*). We note that this same quasi-tripolar signature is observed in both the RFX-mod edge plasma as well as in the space plasma. In panel (*e*) we show the parallel component of the current density. This current is carried by the parallel electrons corresponding to the perpendicular magnetic perturbation (not shown). The radial size of the vortex was found to be $r_0 \approx 3\rho_s$. We also note that a second vortex can be seen a few seconds later [22].

4. Current sheets formed in reconnection events

Magnetic reconnection is a basic phenomenon which occurs in magnetized plasmas, and leads to the conversion between magnetic energy and kinetic energy [24]. It takes place at the border of interacting plasma regions, due to the effect of finite resistivity, which allows a change in magnetic field topology and a mixing of the two otherwise separated plasmas. Reconnection

induces the formation of a current sheet aligned with the main magnetic field (guide field).

Reconnection is a typical feature of turbulent environments. Examples are the magnetosheath, that is the turbulent boundary layer which is formed by the interaction of the solar wind flow with the Earth's magnetosphere, located downstream of the bow shock, the solar corona and several laboratory plasmas. In particular, reconnection is known to occur in RFP plasmas during the so-called discrete relaxation events (DREs), which are seen as periodic oscillations of the toroidal field reversal parameter $F = B_\phi(a)/\langle B_\phi \rangle$, where $\langle \ldots \rangle$ is an average over the poloidal cross-section.

The U-probe has been recently used in the RFX-mod experiment to detect the current sheets produced in DREs [25]. The toroidal array of magnetic probes shows that at the DRE a strong $m = 0$ structure forms at a certain toroidal location, and then propagates toroidally. This is attributed to a poloidal current ring which represents the reconnecting current sheet. During the propagation, a diffusion is also observed, so that the current structure is completely damped after approximately one toroidal turn around the torus [25]. The perturbed quantities measured by the U-probe when the current sheet passes by it are shown in the left part of figure 2. A parallel current density perturbation with a magnitude of 30 kA m^{-2} is found. A corresponding increase in the electron temperature of about 10 eV, about 30% of the mean T_e at the measurement location, is observed. A very slight increase in the density is also found. The resulting electron pressure perturbation is 20 Pa. Finally, an energy transfer from the field to the plasma is measured through the computation of the $\boldsymbol{E} \cdot \boldsymbol{j}$ term, confirming that the reconnection event transfers energy to the plasma.

The turbulent magnetosheath spontaneously creates current sheets at the ion inertial length scale [7, 8]. A typical reconnection event measured in the magnetosheath is depicted in the right part of figure 2. The first panel shows the magnetic-field components, plotted in a local current sheet coordinate system (NML), where L is the maximum varying (reconnecting), M the out-of-plane (tangential) and N the normal components. The second panel shows the differential energy flux (dEF), which indicates that the electron thermal energy (roughly the maximum energy of dEF) increases at the current sheet. The crossing is close to the magnetic null, seen in panel (*c*), where also the density is plotted. This particular current sheet is bifurcated, evident from the out-of-plane current density in panel (*d*), also visible in panel (*a*). The electromagnetic energy is dissipated into particle thermal and kinetic energy, quantified in $\boldsymbol{E} \cdot \boldsymbol{j} > 0$, panel (*e*).

5. Current filaments during edge localized modes

Edge localized modes (ELMs) are short breakdowns of the high confinement regime (H-mode) in tokamaks, which give rise to high energy fluxes on the plasma facing components. Present theories suggest that they originate from a combination of pressure gradient driven MHD modes (ballooning) and edge current density gradient driven modes (peeling modes), which combine in originating intermediate mode number structures ($n \cong 10$–15) well localized in the perpendicular plane but extended along the field lines [26–28]. These structures are then found to propagate in the SOL, where they have been measured using Langmuir probes [29, 30], magnetic pick-up coils [26, 28] or gas puff imaging [31, 32]. The simultaneous investigation of electrostatic and magnetic turbulence associated with ELMs, performed on the ASDEX Upgrade tokamak using the aforementioned probe, offers an interesting opportunity for elucidating the electromagnetic properties of ELMs, in search of signatures for current structures associated with single ELM filaments.

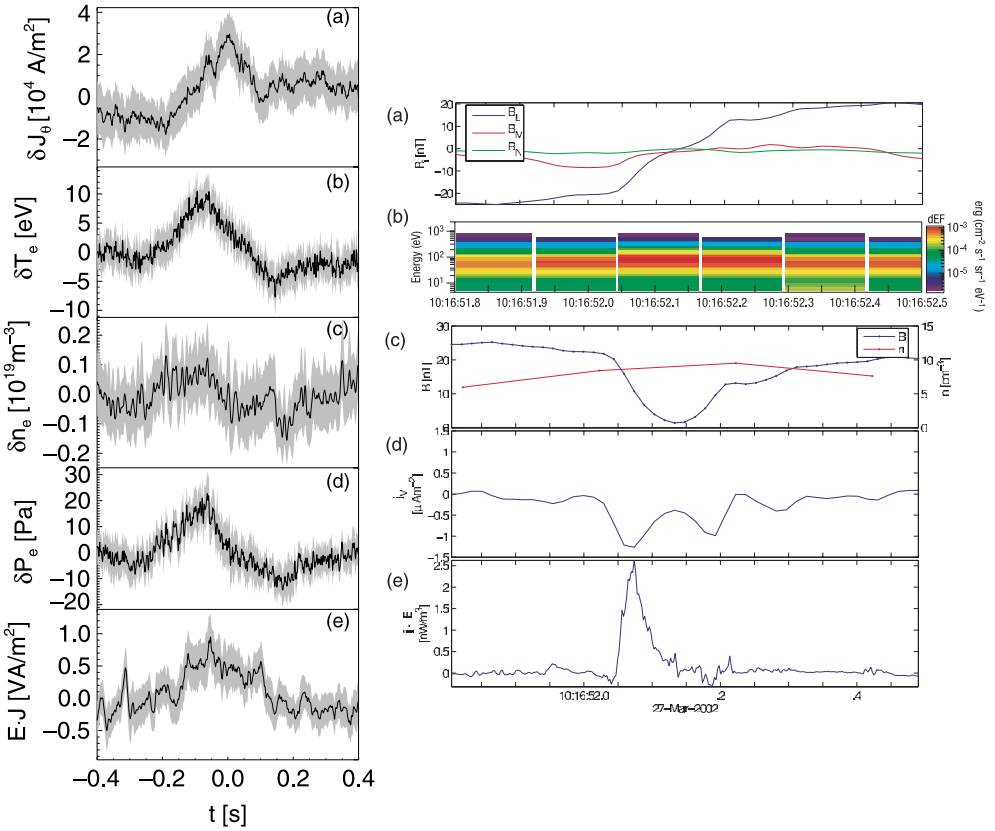

Figure 2. (Left) Perturbation of plasma edge properties in RFX-mod during current sheet transit measured by means of the U-probe at $r/a \simeq 0.9$. From top to bottom are shown the perturbations on (*a*) parallel current density, (*b*) electron temperature, (*c*) plasma density, (*d*) electron pressure, (*e*) energy dissipation. (Right) Reconnection event observed by the Cluster mission in the magnetosheath. From top to bottom are shown (*a*) three components of the magnetic field, (*b*) electron differential flux, (*c*) density and total magnetic field, (*d*) out-of-plane current density, (*e*) energy dissipation.

During the analysis we have used the ion saturation current as collected from one of the probe's tips to infer the passing of the ELM structure in front of the probe [29]. Indeed it is a well-known feature [29, 33] that during the passing of an ELM an abrupt increase in the ion saturation current is measured. This can be recognized in the top panel of figure 3, where eight sharp increases in ion saturation current can be observed, corresponding to eight different ELMs [34]. Approximating the radial velocity with the corresponding $\boldsymbol{E} \times \boldsymbol{B}$ component, and neglecting temperature fluctuations in the determination of the poloidal electric field from the floating potential measurements and of the density from the ion saturation current measurement, we can also compute the instantaneous turbulence-driven particle flux $\Gamma_r = \tilde{n}\tilde{v}_r = \tilde{j}_s\tilde{E}_\theta/B_\phi$ and the corresponding time integral $\int \Gamma_r(t)\,\mathrm{d}t$, which gives an insight into the temporal increase of the radially transported particles. The estimate of $\int \Gamma_r$ is shown in the lower panel of figure 3. It clearly demonstrates the sharp increase in outward fluxes during ELMs. A closer zoom on one of the detected events is reported in figure 4. In panel (*a*) a zoom on the ion saturation current is shown, whereas in panel (*b*) the radial and poloidal components of the magnetic field are plotted. These two components correspond approximately to the perpendicular ones.

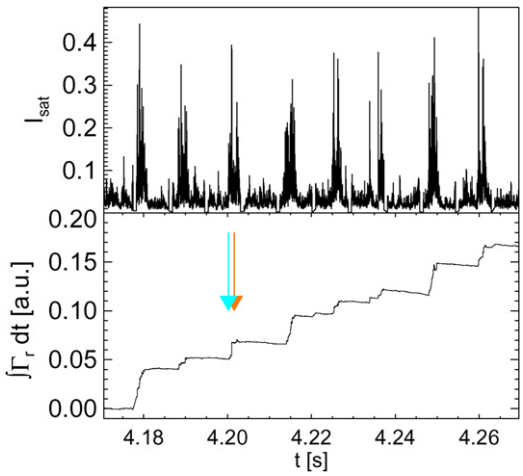

Figure 3. (Top) Ion saturation current during the entire probe insertion. (Bottom) Time-integrated particle flux $\int \Gamma_r \, dt$. The two arrows correspond to the shaded time intervals shown in figure 4.

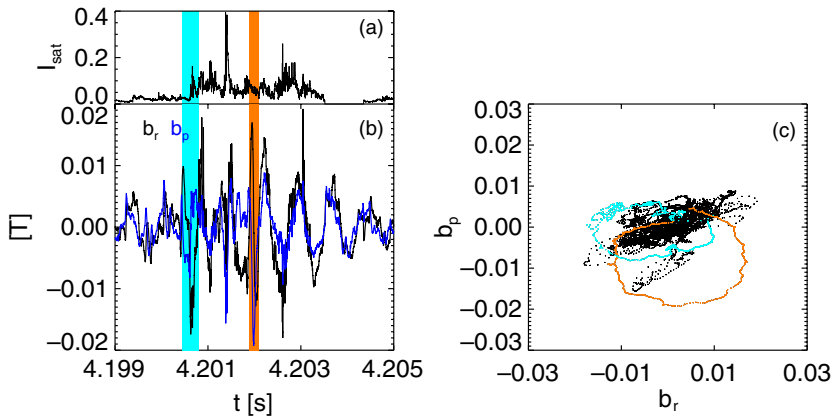

Figure 4. (*a*) Ion saturation current measured in zoomed window, (*b*) radial and poloidal component of the magnetic field, (*c*) hodogram of the perpendicular magnetic field. The two highlighted closed loops correspond to the highlighted time windows in panels (*a*) and (*b*).

It can be clearly observed that when the ion saturation current increases, correspondingly the magnetic activity also increases. The relationship between magnetic activity and ion saturation current bursts is not one-to-one, in agreement with previous observations [27]. Corresponding to the increase in magnetic activity, the radial and poloidal components change their phase relation, moving from approximately in phase to approximately in quadrature, as highlighted by the two shaded regions. This can also be appreciated by looking at the hodogram of the two components, i.e. by considering the magnetic field perturbation trajectory in the b_r–b_p plane. Indeed the shaded regions are associated with closed loops, whereas outside the ELM the magnetic field exhibits an almost linear polarization in the perpendicular plane. Closed loops in the hodograms are compatible with the passing of a current filament, as expected from ELM theories. Using all the three components of the magnetic field it is possible to reconstruct the 3D hodogram shown in figure 5, corresponding to the second shaded interval of figure 4. The trajectory spans a well-defined ellipse lying in a plane. It is possible to compute the

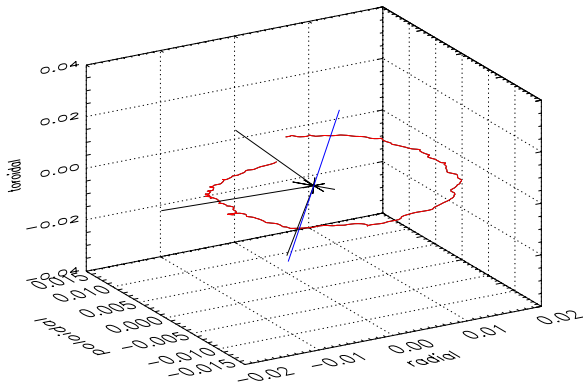

Figure 5. 3D hodogram of the magnetic perturbation associated with an ELM filament. The direction normal to the plane where the ellipse lies is shown together with the direction of the equilibrium magnetic field in a blue line.

direction perpendicular to this plane (shown in figure 5 by a black line), and this is found to correspond to the direction of the equilibrium magnetic field, shown in the same figure by a blue line. This is a further indication of the existence of a parallel current filament associated with an ELM [35].

6. Conclusions

In this paper we have shown how, by using multi-point *in situ* magnetic field measurements, a direct evaluation of current density perturbations can be made. This information, supplemented by Langmuir probe measurements, allows a careful characterization of the phenomena under study, giving a great amount of information. As examples, we have discussed three important topics: DKA vortices measured both in laboratory and magnetospheric plasmas; reconnection events, again both in a laboratory plasma and in the magnetosheath; and current filaments occurring during ELMs in tokamaks (in this latter case a single point magnetic measurement has been used). The results confirm the relevance of this technique, and in general the importance of considering the electromagnetic aspects of turbulent phenomena.

Acknowledgments

This work, supported by the European Communities under the contracts of Association between EURATOM and ENEA, the Austrian Academy of Sciences, the Max Planck Institute for Plasma Physics in Garching and Risø/Danish Technical University, was carried out within the framework of the European Fusion Development Agreement. It was also supported by project P19901 of the Austrian Science Fund (FWF).

References

[1] Frisch U 1995 *Turbulence: The Legacy of A N Kolgomorov* (Cambridge: Cambridge University Press)
[2] Marsch E and Tu C Y 1994 *Ann. Geophys.* **12** 1127
[3] Carbone V, Regnoli G, Martines E and Antoni V 2000 *Phys. Plasmas* **7** 445
[4] Carbone V, Sorriso-Valvo L, Martines E, Antoni V and Veltri P 2000 *Phys. Rev.* E **62** R49
[5] Lorenzini R *et al* 2009 *Nature Phys.* **5** 570

[6] Herrmann A and Gruber O 2003 *Fusion Sci. Technol.* **44** 569
[7] Retinò A, Sundkvist D, Vaivads, A, Mozer F, André M and Owen C J 2007 *Nature Phys.* **3** 235
[8] Sundkvist D, Retinò A, Vaivads A and Bale S D 2007 *Phys. Rev. Lett.* **99** 025004
[9] Spolaore M *et al* 2009 *J. Nucl. Mater.* **390–391** 448
[10] Tsui H Y W *et al* 1992 *Rev. Sci. Instrum.* **63** 4608
[11] Hidalgo C *et al* 1999 *Phys. Rev. Lett.* **83** 2203
[12] Escoubet C P, Schmidt R and Goldstein M L 1997 *Space Sci. Rev.* **79** 11
[13] Hasegawa A and Chen L 1976 *Phys. Fluids* **19** 1924
[14] Stasiewicz K *et al* 2000 *Space Sci. Rev.* **92** 423
[15] Scott B D 2003 *Plasma Phys. Control. Fusion* **45** A385
[16] Scott B D 1997 *Plasma Phys. Control. Fusion* **39** 1635
[17] Shukla P, Yu M and Stenflo L 1986 *Phys. Rev.* A **34** 3478
[18] Petviashvili V I and Pokhotelov O A 1992 *Solitary Waves in Plasmas and in the Atmosphere* (New York: Gordon and Breach)
[19] Vianello N *et al* 2009 Drift-Alfvén vortex structure in the edge region of a fusion relevant plasma arXiv:0904.4831
[20] Spolaore M *et al* 2009 *Phys. Rev. Lett.* **102** 165001
[21] Sundkvist D *et al* 2005 *Nature* **436** 825
[22] Sundkvist D and Bale S D 2008 *Phys. Rev. Lett.* **101** 065001
[23] Grulke O, Ullrich S, Windisch T and Klinger T 2007 *Plasma Phys. Control. Fusion* **49** B247
[24] White R B 1986 *Rev. Mod. Phys.* **58** 183
[25] Zuin M *et al* 2009 *Plasma Phys. Control. Fusion* **51** 035012
[26] Kirk A *et al* 2006 *Plasma Phys. Control. Fusion* **48** B433
[27] Hermann A *et al* 2007 *J. Nucl. Mater.* **363–365** 528
[28] Naulin V *et al* 2009 JET Report EFD-P(08)41 *Nucl. Fusion* submitted http://www.iop.org/Jet/fulltext/EFDP09005.PDF
[29] Endler M *et al* 2005 *Plasma Phys. Control. Fusion* **47** 219
[30] Leonard A W *et al* 2006 *Plasma Phys. Control. Fusion* **48** A149
[31] Terry J L *et al* 2007 *J. Nucl. Mater.* **363–365** 994
[32] Maqueda R J, Maingi R and NSTX team 2009 *Phys. Plasmas* **16** 056117
[33] Schmid A *et al* 2008 *Plasma Phys. Control. Fusion* **50** 045007
[34] Ionita C *et al* 2009 Simultaneous measurements of electrostatic and magnetic fluctuations in ASDEX Upgrade edge plasma *J. Plasma Fusion Res. Ser.* at press
[35] Vianello N *et al* 2009 Direct observation of current in type 1 ELM filaments on ASDEX Upgrade in preparation